

Mixed-Mode Stress Intensity Factors of a Three-Dimensional Crack in a Bonded Bimaterial

T. Y. Qin^{1*} B. J. Zhu^{1,2} N.A. Noda³

1 College of Science, China Agricultural University, Beijing 100083, P. R. CHINA

2. College of Mechatronic and Information Engineering, Hainan University, Haikou 571737, P. R. CHINA

3. Department of Mechanical Engineering, Kyushu Institute of Technology, Kitakyushu, 804-8550, JAPAN

Abstract

Purpose-This paper aims to calculate the mixed-mode stress intensity factors (SIFs) of a three-dimensional crack meeting the interface in a bimaterial under shear loading by a hypersingular integral equation (HIE) method, And further to assess the accuracy of numerical solutions for the mixed mode SIFs along the crack front.

Design/methodology/approach-A three-dimensional crack modeling is reduced to solving a set of HIEs. Based on the analytical solutions of the singular stress field around the crack front, a numerical method for the HIEs is proposed by a finite-part integral method, where the displacement discontinuities of the crack surface are approximated by the product of basic density functions and polynomials. Using FORTRAN program, numerical solutions of the mixed-mode SIFs of some examples are presented.

Findings-The numerical method is proved to be an effective construction technique. The numerical results show that this numerical technique is successful, and the solution precision is satisfied.

Research limitations/implications-This work takes further steps to improve the fundamental systems of HIE for its application in the fields of arbitrary shape crack problems. Propose several techniques for numerical implementation, which could increase the efficiency and accuracy of computation

Practical implications-Whenever there is a structure containing the three dimensional crack, the analysis method described in this paper can be utilized to find the critical configurations under which the structure may be most vulnerable. In such cases, the strength predictions would be safer if the crack could be taken into account.

Originality/value-This paper is the first to apply HIE method to analyzing the mixed-mode crack meeting the interface in three-dimensional dissimilar materials. Numerical solutions of the mixed-mode SIFs can give the satisfied solution precision.

Keywords Stress intensity factor, Boundary element method, Crack, Composite material, Hypersingular integral equation.

Paper type Research paper

1 Introduction

In recent decades, the use of new materials is increasing in a wide range of engineering field and the

* Corresponding author: Tel: +86-10-62736992 Fax: +86-10-62736777
E-mail address: tyqin@cau.edu.cn

accurate evaluation of interface strength in dissimilar materials becomes very important. Considerable researches have been done to evaluate the stress intensity factors and crack opening displacement for cracks in dissimilar materials (Cook and Erdogan, 1972; Lee and Keer, 1986; Chen and Nisitani, 1993; Ang and Fan, 2004). However, most of these works are on two-dimensional cases. Because of the difficulty of mathematics, there are a few analytical methods for three-dimensional crack problems. Antipov (1999) reduced the semi-infinite plane interface crack between 3D isotropic half-spaces to the analysis of 3×3 matrix Wiener-Hopf problem, and found the stresses, discontinuities of the displacements, the stress intensity factors and the weight functions. Using modified integral equation method, Roy and Saha (2000) derived the crack opening displacement of an elliptic crack in an infinite elastic medium subjected to a concentrated pair of point force loading at an arbitrary location on the crack faces and obtain the stress intensity factor along the crack front. However several numerical methods are available, such as the hypersingular integral equation method combined with boundary element method (Qin *et al.* 1997; Helsing *et al.* 2001; Lee and Keer, 1986) evaluated the stress intensity factors of a crack meeting the interface by a body force method, but they didn't give the singularity and the singular stress field near the crack front at the interface. Noda *et al.* (1999) studied mixed mode stress intensity factors of an inclined semi-elliptical surface crack by a body force method, in which the unknown body force densities were approximated by the products of fundamental density functions and polynomials. Qin and Noda (2003) studied a crack meeting the interface in a three-dimensional dissimilar material under a normal load by a hypersingular integral equation method.

In the present paper, a hypersingular integral equation method based on the body force method is applied to solve the problem of a three-dimensional vertical crack meeting at an interface under mixed mode loading. Based on the analytical solution of singular stress field near the crack front, the numerical approach suggested by Noda *et al.* (1999) will be improved to obtain highly reliable numerical results of stress intensity factors.

2 General solutions and the hypersingular integral equation for a planar crack meeting the bimaterial interface

A fixed rectangular Cartesian system x_i ($i=1, 2, 3$) is used. Consider two dissimilar half-spaces bonded together along the x_1-x_3 plane. Suppose that the right half-space (x_2 space) is occupied by an elastic medium with elastic constants (μ_1, ν_1) and the left half-space ($-x_2$ space) is occupied by an elastic medium with elastic constants (μ_2, ν_2) . There is a rectangular crack terminating at the bimaterial interface as shown in Fig.1. The parameters $\theta, \theta_1, \xi_0, r$ and p are the local polar coordinates at the general crack surface, the local polar coordinates at the bimaterial crack surface, source point, distance between the source point and field point and field point, respectively. The crack is assumed to be in a plane normal to the x_3 axis, and subjected to mixed mode loads. Using the Somigliana formula and the body force method (Lee and Keer, 1986), the displacements in the right material can be expressed as

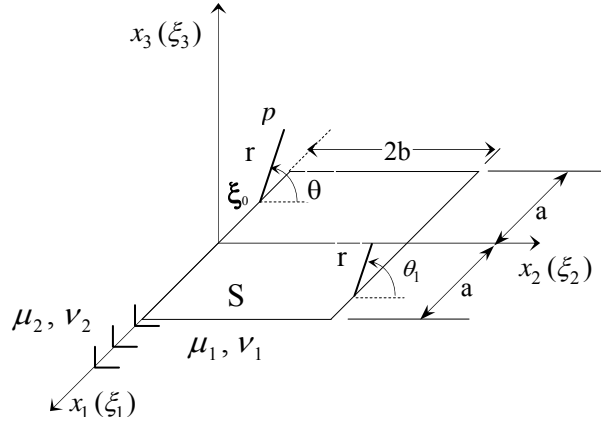


Fig.1 Problem configuration

$$u_i(\mathbf{x}) = \int_S T_{ij}(\mathbf{x}, \boldsymbol{\xi}) \tilde{u}_j(\boldsymbol{\xi}) ds(\boldsymbol{\xi}) \quad i, j=1,2,3 \quad (1)$$

Where $\boldsymbol{\xi}$, \mathbf{x} , and $\tilde{u}_i = u_i^+ - u_i^-$ denote the source point, field point and the i th displacement discontinuity of the crack surface, respectively. The basic solution of stress, $T_{ij}(\mathbf{x}, \boldsymbol{\xi})$, is shown in Appendix. The corresponding stress field is given as follow

$$\sigma_{ij}(\mathbf{x}) = \int_S \left\{ \frac{2\mu_1\nu_1}{1-2\nu_1} \frac{\partial T_{kl}(\mathbf{x}, \boldsymbol{\xi})}{\partial x_k} \delta_{ij} + \mu_1 \left[\frac{\partial T_{il}(\mathbf{x}, \boldsymbol{\xi})}{\partial x_j} + \frac{\partial T_{jl}(\mathbf{x}, \boldsymbol{\xi})}{\partial x_i} \right] \right\} \tilde{u}_l(\boldsymbol{\xi}) ds(\boldsymbol{\xi}) \quad i, j, k, l=1,2,3 \quad (2)$$

Let the point \mathbf{x} in equation (2) tends to the crack surface, using the traction boundary condition of the crack surface, the hypersingular integral equation for unknown function \tilde{u}_i can be obtained

$$\frac{\mu_1}{\pi(\kappa_1 + 1)} \oint_S \left[\frac{\kappa_1 - 1}{2r_1^3} \delta_{\alpha\beta} + \frac{3(3 - \kappa_1)}{4r_1^3} r_{1,\alpha} r_{1,\beta} + K_{\alpha\beta}(\mathbf{x}, \boldsymbol{\xi}) \right] \tilde{u}_\beta(\boldsymbol{\xi}) ds(\boldsymbol{\xi}) = -p_\alpha(\mathbf{x}) \quad \alpha, \beta=1, 2 \quad \mathbf{x} \in S \quad (3)$$

$$\frac{\mu_1}{\pi(\kappa_1 + 1)} \oint_S \left[-\frac{1}{r_1^3} + K_0(\mathbf{x}, \boldsymbol{\xi}) \right] \tilde{u}_3(\boldsymbol{\xi}) ds(\boldsymbol{\xi}) = -p_3(\mathbf{x}) \quad (4)$$

Where \oint is the symbol of the finite-part integral, and

$$K_{11}(\mathbf{x}, \boldsymbol{\xi}) = \frac{2A\kappa_1(\kappa_1 + 6) + 2B - 5C}{4r_2^3} - \frac{24Ax_2\xi_2}{r_2^5} - \frac{3(4A\kappa_1 - C)(x_2 + \xi_2)^2}{4r_2^5} + \frac{30Ax_2\xi_2(x_2 + \xi_2)^2}{r_2^7} - \frac{3(2A\kappa_1 + A\kappa_1^2 + B - 2C)}{2r_2r_3^2} \quad (5)$$

$$K_{12}(\mathbf{x}, \boldsymbol{\xi}) = (x_1 - \xi_1) \left[\frac{3C(x_2 + \xi_2)}{4r_2^5} + \frac{30Ax_2\xi_2(x_2 + \xi_2)}{r_2^7} + \frac{3A(\kappa_1 - 1)x_2}{r_2^5} + \frac{1}{2}(A\kappa_1 + B - C) \left(\frac{1}{r_2^2 r_3^2} + \frac{1}{r_2^3 r_3} \right) \right] \quad (6)$$

$$K_{21}(\mathbf{x}, \boldsymbol{\xi}) = (x_1 - \xi_1) \left[\frac{3(4A + 4A\kappa_1 - C)(x_2 + \xi_2)}{4r_2^5} + \frac{3A(\kappa_1 - 1)x_2}{r_2^5} - \frac{30Ax_2\xi_2(x_2 + \xi_2)}{r_2^7} \right. \\ \left. - \frac{1}{2}(A\kappa_1 + B - C) \left(\frac{1}{r_2^2 r_3^2} + \frac{1}{r_2^3 r_3} \right) \right] \quad (7)$$

$$K_{22}(\mathbf{x}, \boldsymbol{\xi}) = \frac{A + B - C}{2r_2^3} + \frac{3(C - 4A)(x_2 + \xi_2)^2}{4r_2^5} + \frac{24Ax_2\xi_2}{r_2^5} - \frac{30Ax_2\xi_2(x_1 - \xi_1)^2}{r_2^7} \quad (8)$$

$$K_0(\mathbf{x}, \boldsymbol{\xi}) = \frac{2S(\kappa_1 + 1) - 3A(\kappa_1^2 - 2\kappa_1 + 3)}{2r_2^3} + \frac{3A[12x_2\xi_2 - (3 - \kappa_1)(\kappa_1 - 1)(x_2 + \xi_2)^2]}{2r_2^5} \\ + \frac{3(B - 2S + 2A\kappa_1 + A\kappa_1^2 - 2S\kappa_1)}{2r_2 r_3^2} \quad (9)$$

In which $p_i(\mathbf{x})$ denotes the i th direction force at source point \mathbf{x} , $r_{1,\alpha} = (x_\alpha - \xi_\alpha)/r_1$, $r_{1,\beta} = (x_\beta - \xi_\beta)/r_1$, $r_1 = \sqrt{(x_1 - \xi_1)^2 + (x_2 - \xi_2)^2}$, $r_2 = \sqrt{(x_1 - \xi_1)^2 + (x_2 + \xi_2)^2}$. Notice that equations (3, 4) are hypersingular integral equations, and can be numerically solved.

3 Singular indexes near the crack front meeting the interface and intensity factors

According to the theory of the hypersingular integral equation (Cook and Erdogan, 1972; **Qin and Noda, 2002**), the displacement discontinuities of the crack surface near a point $\boldsymbol{\xi}_0$ at the interface can be assumed as

$$\tilde{u}_1(\boldsymbol{\xi}) = D_1(\boldsymbol{\xi}_0) \xi_2^{\lambda_1} \quad 0 < \text{Re}(\lambda_1) < 1 \quad (10)$$

$$\tilde{u}_\alpha(\boldsymbol{\xi}) = D_\alpha(\boldsymbol{\xi}_0) \xi_2^\lambda \quad \alpha = 2, 3 \quad 0 < \text{Re}(\lambda) < 1 \quad (11)$$

where $D_1(\boldsymbol{\xi}_0)$, $D_2(\boldsymbol{\xi}_0)$, and $D_3(\boldsymbol{\xi}_0)$ are non-zero constants related to point $\boldsymbol{\xi}_0$, λ and λ_1 are the stress singular indexes near the crack front meeting the interface, which can be determined by the following equations (Qin and Noda, 2003).

$$\cos(\lambda_1 \pi) = S \quad (12)$$

$$4A\lambda^2 + 2\cos(\lambda\pi) - A - B = 0 \quad (13)$$

The stress intensity factors along the crack front meeting the interface are defined as

$$K_{I,\lambda} = \lim_{r \rightarrow 0} \sigma_{33}(r, \theta)_{|\theta=\pi} (2r)^{1-\lambda} \quad (14)$$

$$K_{II,\lambda} = \lim_{r \rightarrow 0} \sigma_{23}(r, \theta)_{|\theta=\pi} (2r)^{1-\lambda} \quad (15)$$

$$K_{III,\lambda_1} = \lim_{r \rightarrow 0} \sigma_{13}(r, \theta)_{|\theta=\pi} (2r)^{1-\lambda_1} \quad (16)$$

Based on the analytical solutions of the singular stress field around the crack front terminating at the interface (Qin and Noda, 2003), for a point p near the crack front point $\boldsymbol{\xi}_0$ in the right material, the stress intensity factors along the crack front meeting the interface can be rewritten as follow

$$K_{I,\lambda} = \frac{2^{1-\lambda} \mu_1 \lambda \omega D_3(\boldsymbol{\xi}_0)}{(1 + \kappa_1) \sin(\lambda\pi)} = \lim_{\xi_2 \rightarrow 0} \frac{2^{1-\lambda} \lambda \mu_1 \omega \tilde{u}_3}{(\kappa_1 + 1) \sin \lambda \pi \xi_2^\lambda} \quad (17)$$

$$K_{II,\lambda} = \frac{2^{1-\lambda} \mu_1 \lambda \omega D_2(\boldsymbol{\xi}_0)}{(1 + \kappa_1) \sin(\lambda\pi)} = \lim_{\xi_2 \rightarrow 0} \frac{2^{1-\lambda} \lambda \mu_1 \omega \tilde{u}_2}{(\kappa_1 + 1) \sin \lambda \pi \xi_2^\lambda} \quad (18)$$

$$K_{III,\lambda_1} = \frac{2^{1-\lambda_1} \mu_1 \mu_2 \lambda_1 D_1(\xi_0)}{(\mu_1 + \mu_2) \sin(\lambda_1 \pi)} = \lim_{\xi_2 \rightarrow 0} \frac{2^{1-\lambda_1} \mu_1 \mu_2 \tilde{u}_1}{(\mu_1 + \mu_2) \sin(\lambda_1 \pi) \xi_2^{\lambda_1}} \quad (19)$$

Here $\omega = [2 - A - B - 2\lambda(A - B)]$.

4 Numerical procedures

The numerical procedure for equations (4) has been given by Qin and Noda (2003). Here the numerical method for equation (3) will be given as follows. Using the behavior near the crack front, the displacement discontinuities of a rectangular crack can be written as

$$\tilde{u}_1(\xi_1, \xi_2) = F_1(\xi_1, \xi_2) \xi_2^{\lambda_1} \sqrt{(a^2 - \xi_1^2)(2b - \xi_2)} \quad (20)$$

$$\tilde{u}_2(\xi_1, \xi_2) = F_2(\xi_1, \xi_2) \xi_2^{\lambda_2} \sqrt{(a^2 - \xi_1^2)(2b - \xi_2)} \quad (21)$$

To solve the unknown function \tilde{u}_α , the unknown function $F_\alpha(\xi_1, \xi_2)$ is approximately expressed as

$$F_\alpha(\xi_1, \xi_2) = \sum_{m=0}^M \sum_{n=0}^N a_{\alpha mn} \xi_1^m \xi_2^n \quad \alpha = 1, 2 \quad (22)$$

Where $a_{\alpha mn}$ are unknown constants. Substituting (20~21) into (3), a set of algebraic linear equations for unknowns $a_{\alpha mn}$ can be obtained as

$$\sum_{m=0}^M \sum_{n=0}^N a_{\beta mn} I_{\alpha\beta mn}(x_1, x_2) = -\frac{\pi(\kappa_1 + 1)}{\mu_1} p_\alpha(x_1, x_2) \quad (23)$$

Where

$$I_{\alpha\beta mn}(x_1, x_2) = I_{\alpha\beta mn}^1(x_1, x_2) + I_{\alpha\beta mn}^2(x_1, x_2) \quad (24)$$

In which

$$I_{11mn}^1 = \oint_S \frac{1}{4r_1^3} [2(\kappa_1 - 1) + 3(3 - \kappa_1)r_{1,1}^2] \xi_1^m \xi_2^{\lambda_1+n} \sqrt{(a^2 - \xi_1^2)(2b - \xi_2)} d\xi_1 d\xi_2 \quad (25)$$

$$I_{22mn}^1 = \oint_S \frac{1}{4r_1^3} [2(\kappa_1 - 1) + 3(3 - \kappa_1)r_{1,2}^2] \xi_1^m \xi_2^{\lambda_2+n} \sqrt{(a^2 - \xi_1^2)(2b - \xi_2)} d\xi_1 d\xi_2 \quad (26)$$

$$I_{12mn}^1 = \oint_S \frac{3(3 - \kappa_1)}{4r_1^3} r_{1,1} r_{1,2} \xi_1^m \xi_2^{\lambda_1+n} \sqrt{(a^2 - \xi_1^2)(2b - \xi_2)} d\xi_1 d\xi_2 \quad (27)$$

$$I_{21mn}^1 = \oint_S \frac{3(3 - \kappa_1)}{4r_1^3} r_{1,1} r_{1,2} \xi_1^m \xi_2^{\lambda_2+n} \sqrt{(a^2 - \xi_1^2)(2b - \xi_2)} d\xi_1 d\xi_2 \quad (28)$$

$$I_{\alpha 1 mn}^2 = \int_S K_{\alpha 1}(\mathbf{x}, \boldsymbol{\xi}) \xi_1^m \xi_2^{\lambda_1+n} \sqrt{(a^2 - \xi_1^2)(2b - \xi_2)} d\xi_1 d\xi_2 \quad (29)$$

$$I_{\alpha 2 mn}^2 = \int_S K_{\alpha 2}(\mathbf{x}, \boldsymbol{\xi}) \xi_1^m \xi_2^{\lambda_2+n} \sqrt{(a^2 - \xi_1^2)(2b - \xi_2)} d\xi_1 d\xi_2 \quad (30)$$

The integrals (29~30) are general ones, and can be numerically calculated. The integral (25~28) are hypersingulars, and must be treated before being numerically evaluated. Using the Taylor's expansion and the polar coordinates $\xi_1 - x_1 = r_1 \cos \theta_1$, $\xi_2 - x_2 = r_1 \sin \theta_1$ as shown in Figure2, following relations can be obtained

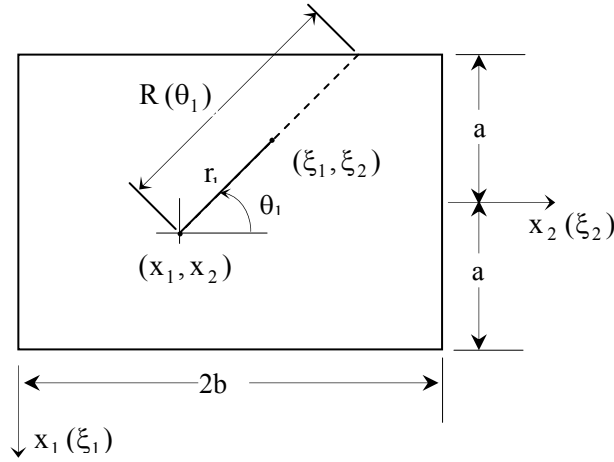


Fig.2 Integral parameters

$$\xi_1^m \sqrt{a^2 - \xi_1^2} = \begin{cases} \sqrt{a^2 - x_1^2} - \frac{x_1}{\sqrt{a^2 - x_1^2}} r_1 \cos \theta_1 - Q_1(x_1, \xi_1, \theta_1) r_1^2, & m=0 \\ x_1^m \sqrt{a^2 - x_1^2} + \frac{x_1^{m-1}}{\sqrt{a^2 - x_1^2}} [ma^2 - (m+1)x_1^2] r_1 \cos \theta_1 + Q_2(x_1, \xi_1, \theta_1) r_1^2, & m>0 \end{cases} \quad (31)$$

$$\xi_2^{\lambda+n} \sqrt{2b - \xi_2} = x_2^{\lambda+n} \sqrt{2b - x_2} + \frac{x_2^{\lambda+n-1}}{2\sqrt{2b - x_2}} [4b(\lambda+n) - (2\lambda+2n+1)x_2] r_1 \sin \theta_1 + Q_3(x_2, \xi_2, \theta_1) r_1^2 \quad (32)$$

Where

$$Q_1 = \frac{a^2(x_1 + \xi_1)}{\sqrt{a^2 - x_1^2} (\sqrt{a^2 - x_1^2} + \sqrt{a^2 - \xi_1^2}) (\xi_1 \sqrt{a^2 - x_1^2} + x_1 \sqrt{a^2 - \xi_1^2})} \cos^2 \theta_1 \quad (33)$$

$$Q_2 = \begin{cases} \frac{1}{2(a^2 - x_1^2)^{3/2}} [m(m-1)a^4 x_1^{m-2} - (2m^2 + 1)a^2 x_1^m + m(m+1)x_1^{m+2}] \cos^2 \theta_1, & \xi_1 = x_1 \\ \frac{1}{r_1^2} \left\{ \xi_1^m \sqrt{a^2 - \xi_1^2} - x_1^m \sqrt{a^2 - x_1^2} - \frac{x_1^{m-1}}{\sqrt{a^2 - x_1^2}} [ma^2 - (m+1)x_1^2] (\xi_1 - x_1) \right\}, & \xi_1 \neq x_1 \end{cases} \quad (34)$$

$$Q_3 = \begin{cases} \frac{x_2^{\lambda+n-2}}{8(2b - x_2)^{3/2}} \{16(\lambda+n)(\lambda+n-1)b^2 - 8b(\lambda+n)(2\lambda+2n-1)x_2 + [4(\lambda+n)^2 - 1]x_2^2\} \sin^2 \theta_1, & \xi_2 = x_2 \\ \frac{1}{r_1^2} \left\{ \xi_2^{\lambda+n} \sqrt{2b - \xi_2} - x_2^{\lambda+n} \sqrt{2b - x_2} - \frac{x_2^{\lambda+n-1}}{2\sqrt{2b - x_2}} [4b(\lambda+n) - (2\lambda+2n+1)x_2] (\xi_2 - x_2) \right\}, & \xi_2 \neq x_2 \end{cases} \quad (35)$$

Using relations (31~32), the kernels of integral (25~28) can be written as follow

$$\xi_1^m \xi_2^{\lambda+n} \sqrt{(a^2 - \xi_1^2)(2b - \xi_2)} = C_0(x_1, x_2) + C_1(x_1, x_2, \theta_1) r_1 + C_2(x_1, x_2, r_1, \theta_1) r_1^2 \quad (36)$$

$$\xi_1^m \xi_2^{\lambda+n} \sqrt{(a^2 - \xi_1^2)(2b - \xi_2)} = D_0(x_1, x_2) + D_1(x_1, x_2, \theta_1) r_1 + D_2(x_1, x_2, r_1, \theta_1) r_1^2 \quad (37)$$

Where $C_i(x_1, x_2)$ and $D_i(x_1, x_2)$ ($i=0, 1, 2$) are known functions, and can be obtained by Taylor's expansion. Using the finite-part integral method and relations (36~37), the hypersingular integrals (25~28) can be reduced as

$$I_{11mn}^1 = \int_0^{2\pi} \frac{1}{4} [2(\kappa_1 - 1) + 3(3 - \kappa_1) \cos^2 \theta_1] \left[-\frac{C_0(x_1, x_2)}{R(\theta_1)} + C_1(x_1, x_2, \theta_1) \ln R(\theta_1) \right. \\ \left. + \int_0^{R(\theta_1)} C_2(x_1, x_2, r_1, \theta_1) dr_1 \right] d\theta_1 \quad (38)$$

$$I_{21mn}^1 = \int_0^{2\pi} \frac{3}{4} (3 - \kappa_1) \sin \theta_1 \cos \theta_1 \left[-\frac{C_0(x_1, x_2)}{R(\theta_1)} + C_1(x_1, x_2, \theta_1) \ln R(\theta_1) \right. \\ \left. + \int_0^{R(\theta_1)} C_2(x_1, x_2, r_1, \theta_1) dr_1 \right] d\theta_1 \quad (39)$$

$$I_{12mn}^1 = \int_0^{2\pi} \frac{3}{4} (3 - \kappa_1) \sin \theta_1 \cos \theta_1 \left[-\frac{D_0(x_1, x_2)}{R(\theta_1)} + D_1(x_1, x_2, \theta_1) \ln R(\theta_1) \right. \\ \left. + \int_0^{R(\theta_1)} D_2(x_1, x_2, r_1, \theta_1) dr_1 \right] d\theta_1 \quad (40)$$

$$I_{22mn}^1 = \int_0^{2\pi} \frac{1}{4} [2(\kappa_1 - 1) + 3(3 - \kappa_1) \sin^2 \theta_1] \left[-\frac{D_0(x_1, x_2)}{R(\theta_1)} + D_1(x_1, x_2, \theta_1) \ln R(\theta_1) \right. \\ \left. + \int_0^{R(\theta_1)} D_2(x_1, x_2, r_1, \theta_1) dr_1 \right] d\theta_1 \quad (41)$$

Now the integrals in (38~41) are generals, and can be calculated numerically. From (15~16) and (18~22), the stress intensity factors at the crack front point x_0 on the interface can be evaluated as follow

$$K_{II, \lambda} = \frac{2^{1-\lambda} \lambda \mu_1 \omega}{(\kappa_1 + 1) \sin \lambda \pi} \sqrt{2b(a^2 - x_1^2)} F_2(x_1, 0) \quad -a \leq x_1 \leq a \quad (42)$$

$$K_{III, \lambda_1} = \frac{2^{1-\lambda_1} \mu_1 \mu_2}{(\mu_1 + \mu_2) \sin(\lambda_1 \pi)} \sqrt{2b(a^2 - x_1^2)} F_1(x_1, 0) \quad -a \leq x_1 \leq a \quad (43)$$

5 Numerical results

Consider a rectangular crack meeting the interface in three-dimensional infinite dissimilar material body under a uniform shear load σ_{31}^∞ or σ_{32}^∞ at infinity. In demonstrating the numerical results, the following dimensionless stress intensity factors of the interface crack front and inner crack front will be used

$$F_{3, \lambda_1} = K_{III, \lambda_1} / \sigma_{31}^\infty b^{1-\lambda_1} \quad F_{2, \lambda} = K_{II, \lambda} / \sigma_{31}^\infty b^{1-\lambda} \quad (44)$$

$$F_2 = K_{II} / \sigma_{31}^\infty \sqrt{b} \quad F_3 = K_{III} / \sigma_{31}^\infty \sqrt{b} \quad (45)$$

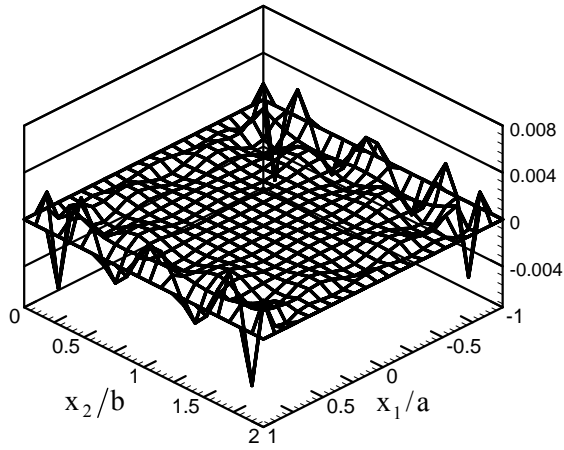
If the load is σ_{32}^∞ , the load σ_{31}^∞ in (44~45) should be replaced by σ_{32}^∞ .

5.1 Compliance of boundary condition and convergence of numerical solutions

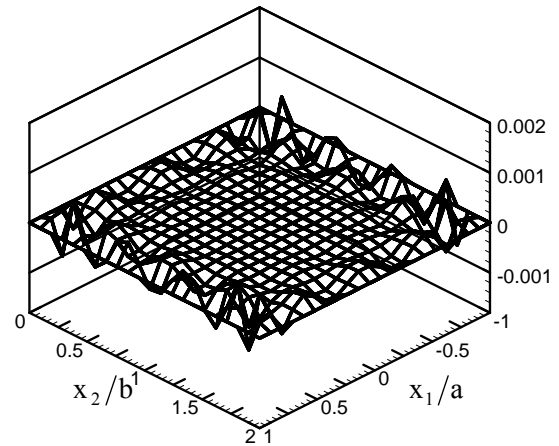
In solving the algebraic equations (23), the least square method is applied to minimize the residual stress at the collocation points. When the solid is subjected to a uniform shear load σ_{31}^∞ at infinity, Figure 3 and Figure 4 show the compliance of the boundary conditions along the crack surface for $a/b=1$, $\mu_2 / \mu_1 = 2$, $\nu_1 = \nu_2 = 0.3$, where the collocation point number is 400 (20×20). For this case, the singular indexes are $\lambda = 0.566$ and $\lambda_1 = 0.608$. It is shown that the remaining stresses

$\left(\frac{\sigma_{31}^\infty}{\sigma_{31}^\infty} + 1\right)$ and $\frac{\sigma_{32}^\infty}{\sigma_{31}^\infty}$ on the crack surface are less than 0.006 when $M=N=7$, less than 4.0×10^{-4}

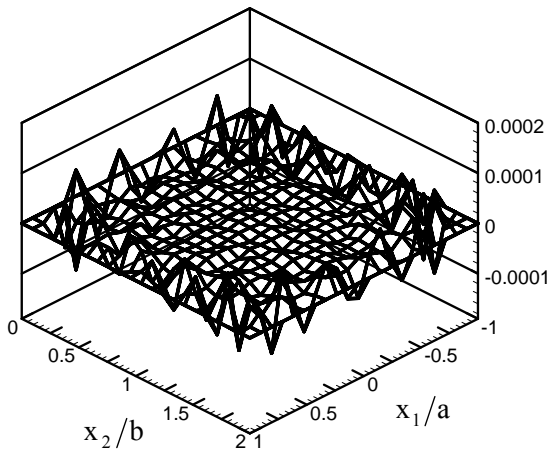
when $M=N=9$, less than 6.0×10^{-5} when $M=N=11$, and less than 1.6×10^{-5} when $M=N=13$.



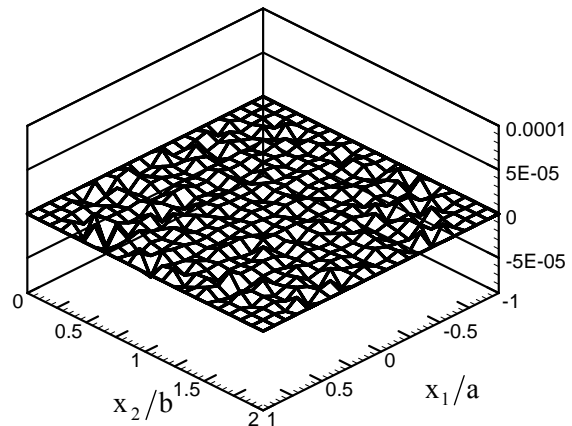
(a) $M=N=7$



(b) $M=N=9$

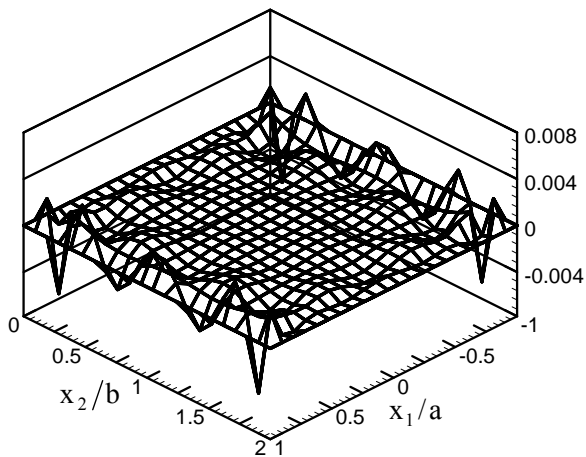


(c) $M=N=11$

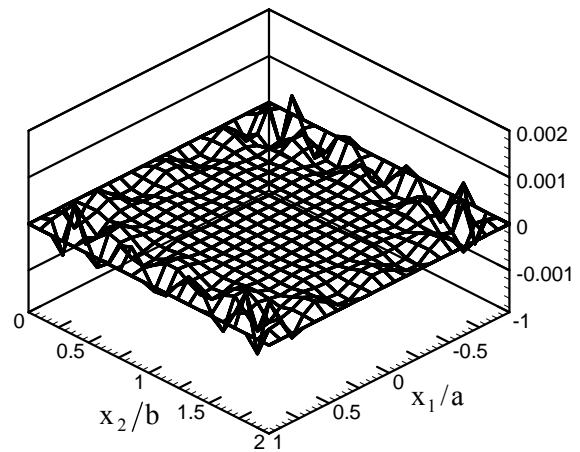


(d) $M=N=13$

Fig.3 Compliance of boundary condition $\frac{\sigma_{31}}{\sigma_{31}^{\infty}} = -1$ when $a/b=1, \mu_2/\mu_1 = 2 \quad \nu_1 = \nu_2 = 0.3$



(a) $M=N=7$



(b) $M=N=9$

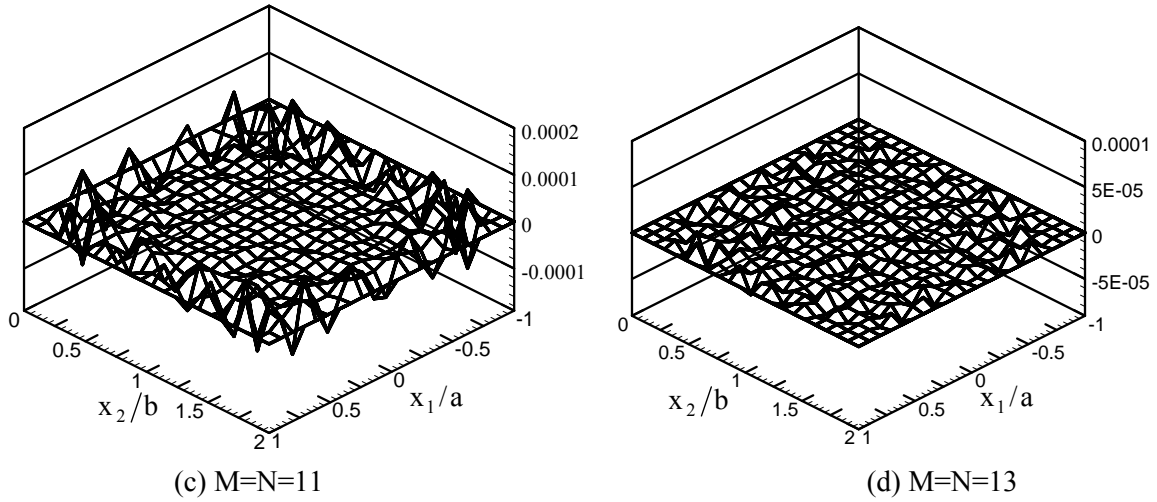


Fig.4 Compliance of boundary condition $\frac{\sigma_{32}}{\sigma_{31}} = 0$ when $a/b=1, \mu_2/\mu_1 = 2, \nu_1 = \nu_2 = 0.3$

In the case of homogeneous materials, the numerical results of dimensionless stress intensity factors with increasing the polynomial exponents are given in Table1 and Table2, and compared with those given by Noda and Kihara (2002) and Chen (2004). Due to the symmetry, only the numerical results for $x_2/b \geq 1$ are given. It is shown that the results are convergent, and the collocation point number 20×20 and the polynomial exponents $M=N=9$ are enough for satisfied result precision in this case. Since the polynomial exponents are larger than that used by Chen (2004), the present results are more reliable. In general, too large polynomial exponents can't give reliable results. The polynomial exponents M, N depend on the collocation point number. For the polynomial exponents $M=N=15$, the results of the collocation point number 20×20 are not good, but the ones of the collocation point number 30×30 are satisfied.

Table 1 Convergence of dimensionless stress intensity factor F_2 along $x_1 = \pm a$ with increasing the polynomial exponents $M=N$ ($a/b=1, \mu_2/\mu_1 = 1, \nu_1 = \nu_2 = 0.3, \text{ Collocation points } 20 \times 20$)

	x_2/b									
	1	1.1	1.2	1.3	1.4	1.5	1.6	1.7	1.8	1.9
M=5	0.8450	0.8424	0.8332	0.8190	0.8004	0.7779	0.7502	0.7122	0.6502	0.5243
M=7	0.8398	0.8382	0.8328	0.8224	0.8049	0.7810	0.7506	0.7058	0.6536	0.5201
M=9	0.8412	0.8391	0.8321	0.8208	0.8042	0.7820	0.7526	0.7051	0.6499	0.5238
M=11	0.8411	0.8390	0.8325	0.8212	0.8041	0.7817	0.7525	0.7054	0.6484	0.5226
M=13	0.8412	0.8391	0.8325	0.8212	0.8041	0.7817	0.7526	0.7058	0.6472	0.5228
Noda	0.8412	0.8391	—	0.8216	—	0.7819	—	0.7062	—	0.5381
Chen	0.8388	0.8375	0.8333	0.8225	0.8122	0.7911	0.7579	0.7056	0.6217	0.4760

Table 2 Convergence of dimensionless stress intensity factor F_{3,λ_1} along $x_2 = 0$ with increasing the polynomial exponents $M=N$ ($a/b=1, \mu_2/\mu_1 = 1, \nu_1 = \nu_2 = 0.3, \text{ Collocation points } 20 \times 20$)

	x_1/a									
	0	0.1	0.2	0.3	0.4	0.5	0.6	0.7	0.8	0.9
M=5	0.6563	0.6542	0.6477	0.6372	0.6224	0.6028	0.5769	0.5402	0.4831	0.3794
M=7	0.6540	0.6523	0.6466	0.6368	0.6219	0.6026	0.5787	0.5402	0.5016	0.4010
M=9	0.6544	0.6524	0.6466	0.6365	0.6216	0.6018	0.5787	0.5362	0.5023	0.4024
M=11	0.6544	0.6524	0.6466	0.6365	0.6217	0.6020	0.5781	0.5370	0.4951	0.4021
M=13	0.6544	0.6525	0.6467	0.6366	0.6217	0.6023	0.5779	0.5372	0.4906	0.4020
Noda	0.6544	0.6525	—	0.6369	—	0.6025	—	0.5389	—	0.4080
Chen	0.6638	0.6619	0.6561	0.6457	0.6296	0.6063	0.5728	0.5248	0.4540	0.3406

5.2 A rectangular surface crack in a half space

If $\mu_2/\mu_1 \rightarrow 0$, it is the case of a surface crack in a half space. Now the polynomial exponents are taken as $M=N=9$, and the collocation point number is 20×20 . For a rectangular surface crack in a homogeneous material, Table 3 gives the maximum stress intensity factor F_3 under a uniform shear load σ_{31}^∞ for different ratios of a/b . It is shown that, for the case of anti-plane problem, present results are close to those given by Westergaard (1939) and Tada (1972). Table 4 gives the maximum stress intensity factor F_2 under a uniform shear load σ_{32}^∞ . It is shown that, for the case of plane problem, present results are close to those given by Tracey and Cook (1977) and Xiao and Karihaloo (2002).

Table 3 Dimensionless stress intensity factor F_3 for $\mu_2/\mu_1 = 0$, $\nu_1 = 0.3$ at $x_1 = 0, x_2 = 2b$

	a/b						
	1	2	5	8	10	12	∞
Present	0.6615	0.8645	1.147	1.285	1.385	1.410	—
Westergaard	—	—	—	—	—	—	1.414
Tada	—	—	—	—	—	—	1.414

Table 4 Dimensionless stress intensity factor F_2 for $\mu_2/\mu_1 = 0$, $\nu_1 = 0.3$ at $x_1 = 0, x_2 = 2b$

	a/b				
	1	2	5	8	∞
Present	0.9703	1.255	1.480	1.542	—
Tracey	—	—	—	—	1.542
Xiao	—	—	—	—	1.539

5.3 Solutions for general cases

For general cases, the polynomial exponents are taken as $M=N=9$, and the collocation point number is 20×20 for the following results. When the solid is subjected to a uniform shear load σ_{31}^∞ at

infinity, the stress intensity factor along the crack front meeting at the interface is of mode III. Table5 gives the maximum stress intensity factor F_{3,λ_1} for different ratios of a/b and μ_2/μ_1 . The dimensionless stress intensity factors F_2 at crack front point (a, b) and F_3 at crack front point (0, 2b) are shown in Figure5 and Figure6 for different ratio of μ_2/μ_1 , respectively. It can be shown that the stress intensity factors vary more gently when $\mu_2/\mu_1 \geq 10$. In case of $\mu_2/\mu_1 = 2$, Figure7 gives the dimensionless stress intensity factor F_{3,λ_1} along the crack front meeting at the interface for different ratios of a/b. Figure 8 gives the dimensionless stress intensity factor F_2 along the interface crack front ($x_1 = \pm a$) for $\nu_1 = \nu_2 = 0.3$ and $\mu_2/\mu_1 = 10$. When the solid is subjected to a uniform shear load σ_{32}^∞ at infinity, the stress intensity factor along the crack front meeting at the interface is of mode II. The dimensionless stress intensity factor $F_{2,\lambda}$ along the crack front meeting at the interface is given graphically in Figure9 for $\mu_2/\mu_1 = 2$ and different ratios of a/b. Figure10 gives the dimensionless stress intensity factor F_3 along the interface crack front ($x_1 = \pm a$) for $\nu_1 = \nu_2 = 0.3$ and $\mu_2/\mu_1 = 2$.

Table 5 Dimensionless stress intensity factor F_{3,λ_1} for $\nu_1 = \nu_2 = 0.3$, at $x_1 = 0, x_2 = 0$

	μ_2/μ_1							
	0.1	0.5	1.0	2.0	5.0	10	20	50
	$(\lambda_1=0.195)$	$(\lambda_1=0.392)$	$(\lambda_1=0.5)$	$(\lambda_1=0.608)$	$(\lambda_1=0.732)$	$(\lambda_1=0.805)$	$(\lambda_1=0.860)$	$(\lambda_1=0.911)$
a/b=1	0.1098	0.3534	0.6544	1.189	2.808	4.652	5.160	5.165
a/b=2	0.1616	0.4452	0.8099	1.479	3.355	5.419	5.928	5.932
a/b=3	0.2276	0.5411	0.9715	1.835	3.803	5.847	6.355	6.359

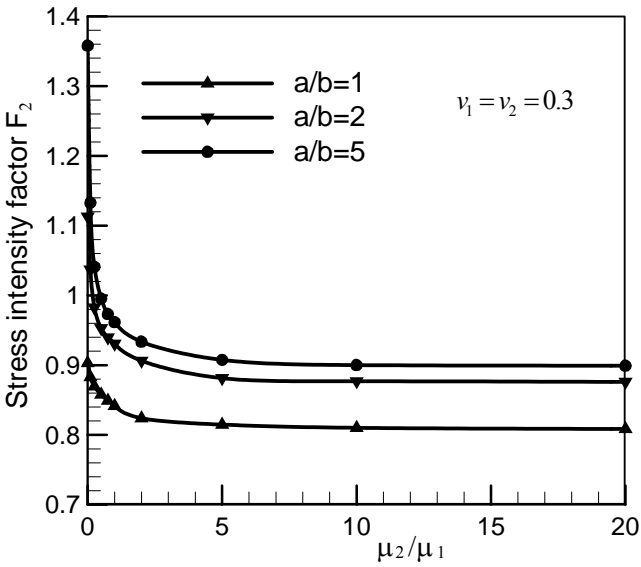


Fig.5 Dimensionless stress intensity factors F_2 at points ($x_1 = \pm a, x_2 = b$),

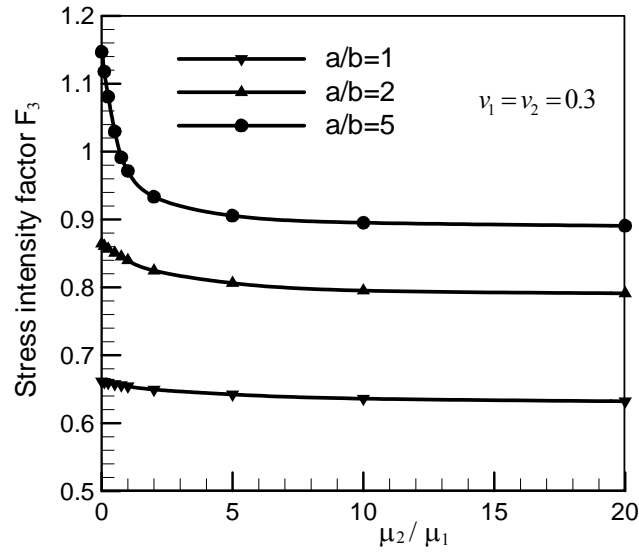


Fig.6 Dimensionless stress intensity factors F_3 at point $(x_1 = 0, x_2 = 2b)$

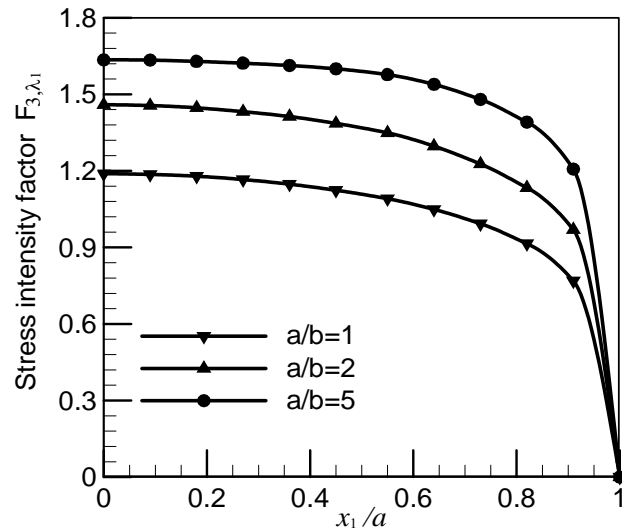


Fig. 7 Dimensionless stress intensity factor F_{3,λ_1} along the interface crack front $(x_2 = 0)$ for $\nu_1 = \nu_2 = 0.3$, $\mu_2/\mu_1 = 2$, $\lambda_1 = 0.608$

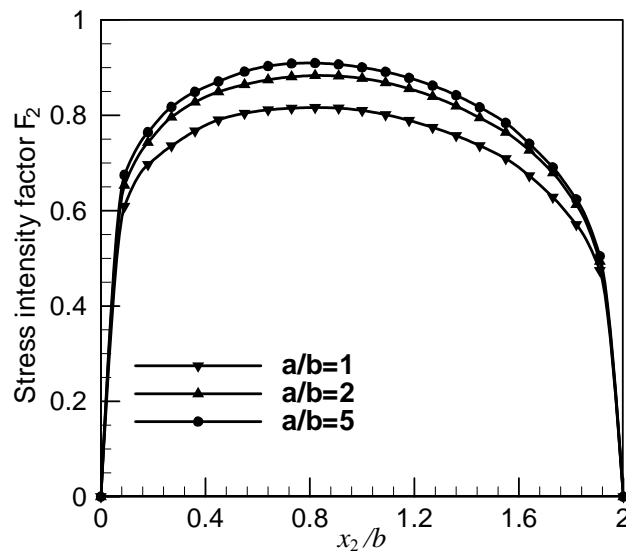


Fig.8 Dimensionless stress intensity factor F_2 along the interface crack front ($x_1 = \pm a$)
for $\nu_1 = \nu_2 = 0.3$, $\mu_2/\mu_1 = 10$

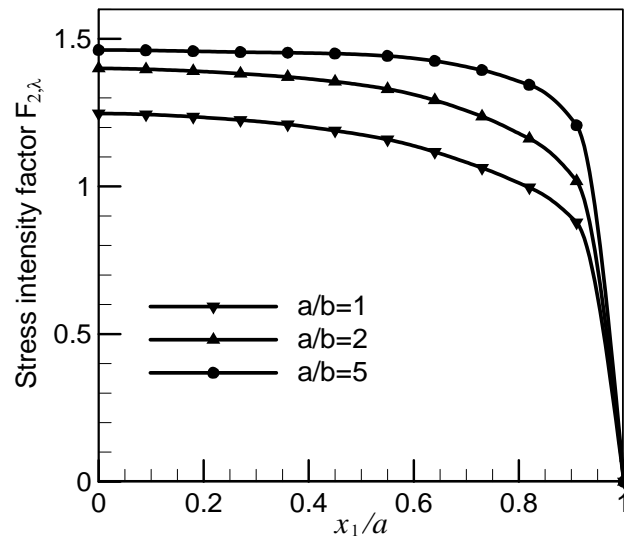


Fig. 9 Dimensionless stress intensity factor $F_{2,\lambda}$ along the interface crack front ($x_2 = 0$)
for $\nu_1 = \nu_2 = 0.3$, $\mu_2/\mu_1 = 2$, $\lambda=0.566$

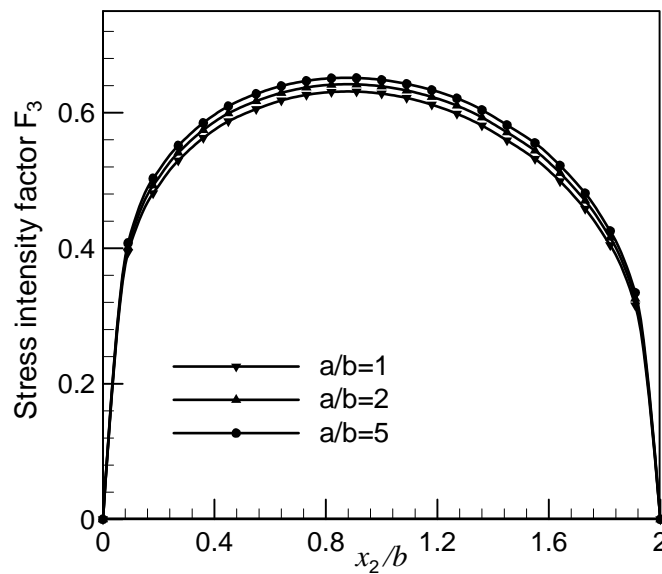


Fig.10 Dimensionless stress intensity factor F_3 along the interface crack front ($x_1 = \pm a$)
for $\nu_1 = \nu_2 = 0.3$, $\mu_2/\mu_1 = 2$

6 Conclusions

A mixed-mode rectangular crack meeting the interface in a three-dimensional dissimilar materials subjected to shear loads is studied by a hypersingular integral equation based on the body force method.

1) The stress singularity and singular stress field around the crack front terminating at the interface are

obtained by the main-part analytical method. Although expressions of the displacements and stresses in the materials are complex in modality, the solutions of singular stresses around the crack front are briefly discussed.

2) The unknown function of the hypersingular integral equation is approximated by a product of a series of power polynomials and a fundamental solution, which exactly expresses the singularities of stresses near the crack front. The numerical results show that this numerical technique is successful, and the solution precision is satisfied.

3) From the numerical solutions, it is shown that the stress intensity factors vary more gently when $\mu_2/\mu_1 \geq 10$, and the stress intensity factor at the center of the crack front for the case of $a/b \geq 8$ is close to that of two-dimensional case.

Acknowledgment

The authors wish to thank the reviewers for the useful comments and suggestions.

Appendix

$$T_{11} = \frac{x_3}{2\pi(\kappa_1 + 1)} \left\{ \frac{(\kappa_1 - 1)}{2r_1^3} + \frac{3(x_1 - \xi_1)^2}{r_1^5} + \frac{C - 2A\kappa_1}{2r_2^3} + \frac{6Ax_2\xi_2}{r_2^5} + \frac{3A\kappa_1(x_1 - \xi_1)^2}{r_2^5} - \frac{30Ax_2\xi_2(x_1 - \xi_1)^2}{r_2^7} \right. \\ \left. + \frac{C}{r_2r_3^2} \left[1 - \frac{2(x_1 - \xi_1)^2}{r_2r_3} - \frac{(x_1 - \xi_1)^2}{r_2^2} \right] \right\} \quad (1)$$

$$T_{21} = \frac{(x_1 - \xi_1)x_3}{2\pi(\kappa_1 + 1)} \left[\frac{3(x_2 - \xi_2)}{r_1^5} + \frac{3A\kappa_1(x_2 - \xi_2)}{r_2^5} - \frac{30Ax_2\xi_2(x_2 + \xi_2)}{r_2^7} + \frac{1}{2}(A\kappa_1^2 - B) \left(\frac{1}{r_2^2r_3^2} + \frac{1}{r_2^3r_3} \right) \right] \quad (2)$$

$$T_{31} = \frac{(x_1 - \xi_1)}{2\pi(\kappa_1 + 1)} \left\{ \frac{\kappa_1 - 1}{2r_1^3} + \frac{3x_3^2}{r_1^5} + \frac{C - 2A\kappa_1}{2r_2^3} + \frac{6Ax_2\xi_2}{r_2^5} + \frac{3A\kappa_1x_3^2}{r_2^5} - \frac{30Ax_2\xi_2x_3^2}{r_2^7} + \frac{C}{r_2r_3^2} \left[1 - \frac{x_3^2}{r_2^2} - \frac{2x_3^2}{r_2r_3} \right] \right\} \quad (3)$$

$$T_{12} = \frac{(x_1 - \xi_1)x_3}{2\pi(\kappa_1 + 1)} \left[\frac{3(x_2 - \xi_2)}{r_1^5} + \frac{3A(\kappa_1 - 1)x_2}{r_2^5} - \frac{3A\kappa_1(x_2 + \xi_2)}{r_2^5} + \frac{30Ax_2\xi_2(x_2 + \xi_2)}{r_2^7} + \frac{1}{2}(A\kappa_1 + B - C) \right. \\ \left. \cdot \left(\frac{1}{r_2^2r_3^2} + \frac{1}{r_2^3r_3} \right) \right] \quad (4)$$

$$T_{22} = \frac{x_3}{2\pi(\kappa_1 + 1)} \left[\frac{3(x_2 - \xi_2)^2}{r_1^5} + \frac{\kappa_1 - 1}{2r_1^5} + \frac{C - A\kappa_1}{r_2^3} - \frac{6Ax_2\xi_2}{r_2^5} - \frac{3A(\kappa_1 + 1)x_2(x_2 + \xi_2)}{r_2^5} + \frac{3A\kappa_1(x_2 + \xi_2)^2}{r_2^5} \right. \\ \left. + \frac{30Ax_2\xi_2(x_2 + \xi_2)}{r_2^7} + \frac{C_1}{2r_2^2} \right] \quad (5)$$

$$T_{32} = \frac{1}{2\pi(\kappa_1 + 1)} \left[\frac{(\kappa_1 - 1)(x_2 - \xi_2)}{2r_1^3} - \frac{A(\kappa_1 - 1)x_2}{r_2^3} - \frac{(C - 2A\kappa_1)(x_2 + \xi_2)}{2r_2^3} - \frac{6Ax_2\xi_2(x_2 + \xi_2)}{r_2^5} + \frac{3A(\kappa_1 - 1)x_2\xi_2}{r_2^5} \right. \\ \left. + \frac{3(x_2 - \xi_2)x_3^2}{r_1^5} - \frac{3A\kappa_1(x_2 + \xi_2)x_3}{r_2^5} - \frac{30Ax_2\xi_2(x_2 + \xi_2)x_3^2}{r_2^7} + \frac{1}{2}(A\kappa_1 + B - C) \left(\frac{1}{r_2r_3} - \frac{x_3^2}{r_2^2r_3^2} - \frac{x_3^2}{r_2^3r_3} \right) \right] \quad (6)$$

$$T_{13}(\mathbf{x}, \boldsymbol{\xi}) = \frac{(x_1 - \xi_1)}{2\pi(\kappa_1 + 1)} \left\{ \frac{1 - \kappa_1}{2r_1^3} + \frac{3x_3^2}{r_1^5} - \frac{A\kappa_1(\kappa_1 - 1)}{2r_2^3} + \frac{6Ax_2\xi_2}{r_2^5} - \frac{3A(3 - \kappa_1)x_2(x_2 + \xi_2)}{r_2^5} \right. \\ \left. + \frac{3A\kappa_1x_3^2}{r_2^5} - \frac{30Ax_2\xi_2x_3^2}{r_2^5} + \frac{1}{2}(A\kappa_1^2 + 2A\kappa_1 + B - 2C) \left(\frac{1}{r_2r_3} - \frac{2x_3^2}{r_2^2r_3^2} - \frac{x_3^2}{r_2^3r_3^2} \right) \right\} \quad (7)$$

$$T_{23}(\mathbf{x}, \boldsymbol{\xi}) = \frac{1}{2\pi(\kappa_1 + 1)} \left\{ (x_2 - \xi_2) \left(\frac{1 - \kappa_1}{2r_1^3} + \frac{3x_3^2}{r_1^5} \right) + \frac{(6A - 5A\kappa_1)(x_2 + \xi_2) + 6A(\kappa_1 - 1)\xi_2}{2r_2^3} \right. \\ \left. + \frac{6Ax_2\xi_2(x_2 + \xi_2)}{r_2^5} - \frac{3A(3 - \kappa_1)x_2(x_2 + \xi_2)^2}{r_2^5} + \frac{3A\kappa_1(x_2 - \xi_2)x_3^2}{r_2^5} \right. \\ \left. - \frac{30Ax_2\xi_2(x_2 + \xi_2)x_3^2}{r_2^5} - \frac{1}{2}(A\kappa_1^2 - B) \left(\frac{1}{r_2r_3} - \frac{x_3^2}{r_2^2r_3^2} - \frac{x_3^2}{r_2^3r_3^2} \right) \right\} \quad (8)$$

$$T_{33}(\mathbf{x}, \boldsymbol{\xi}) = \frac{x_3}{2\pi(\kappa_1 + 1)} \left\{ \frac{\kappa_1 - 1}{2r_1^3} + \frac{3x_3^2}{r_1^5} + \frac{2C - A\kappa_1(3 + \kappa_1)}{2r_2^3} + \frac{18Ax_2\xi_2}{r_2^5} - \frac{3A(3 - \kappa_1)x_2(x_2 + \xi_2)}{r_2^5} \right. \\ \left. + \frac{3A\kappa_1x_3^2}{r_2^5} - \frac{30Ax_2\xi_2x_3^2}{r_2^5} + \frac{1}{2}(A\kappa_1^2 + 2A\kappa_1 + B - 2C) \left(\frac{3}{r_2r_3^2} - \frac{2x_3^2}{r_2^2r_3^3} - \frac{x_3^2}{r_2^3r_3^2} \right) \right\} \quad (9)$$

and

$$r_1 = \sqrt{(x_1 - \xi_1)^2 + (x_2 - \xi_2)^2 + x_3^2}, \quad r_2 = \sqrt{(x_1 - \xi_1)^2 + (x_2 + \xi_2)^2 + x_3^2}, \quad r_3 = r_2 + x_2 + \xi_2$$

$$A = (1 - \Gamma)/(1 + \kappa_1\Gamma), \quad B = (\kappa_2 - \kappa_1\Gamma)/(\Gamma + \kappa_2), \quad S = (1 - \Gamma)/(1 + \Gamma), \quad \Gamma = \mu_2/\mu_1, \quad C = S(\kappa_1 + 1)$$

$$\kappa = 3 - 4\nu, \quad C_1 = \frac{1}{2}(A\kappa_1^2 - B)$$

References

- Antipov Y A. 1999. An exact solution of the 3-D-problem of an interface semi-infinite plane crack. *J. Mech. Phys. Solids*, 47, 1051-1093
- Chen, D. H., Nisitani, H., 1993. Stress intensity factors of a crack meeting the bimaterial interface. *Transactions of the Japanese Society of Mechanical Engineerings* 59 A, 47-53 (in Japanese).
- Chen Y. Z., 2004, Hypersingular integral equation method for three-dimensional crack problem in shear mode. *Commun. Numer. Meth. Engng*; 20:441-454
- Cook, T. S., Erdogan, F. (1972). Stresses in bonded materials with a crack perpendicular to the interface. *Int. J. Eng Sci* 10(8), 677-697.
- Helsing J., Jonsson A., Peters G. 2001. Evaluation of the mode I stress intensity factor for a square crack in 3D. *Engng. Fract. Mech* 68, 605-612.
- Lee, J. C., Keer, L. M., 1986. Study of a three-dimensional crack terminating at an interface. *ASME J. Appl. Mech* 53, 311-316.
- Mukhopahyay N.K., Maiti S. K., Kakodkar. A 1998. BEM based evaluation of SIFs using modified crack closure integral technique under remote and/or crack edge loading. *Engng. Fract. Mech* 61, 655-671
- Noda N.A., Kihara T. A., 2002, Variation of the stress intensity factor along the front of a 3-D rectangular crack subjected to mixed-mode load. *Archive of Applied Mechanics* 72, 599 - 614
- Noda, N. A., Kobayashi, K., Yagishita. M. 1999. Variation of mixed modes stresses intensity factors of

an inclined semi-elliptical surface crack. *Int. J. Fract* 100, 207-225.

Sih G. C., 1965. External crack under longitudinal shear. *J. Franklin Institute* 280 (2), 139-149

Qin T. Y., Chen W. J., Tang R. J., 1997. Three-dimensional crack problem analysis using boundary element method with finite-part integrals. *Int. J. Fract* 84, 191-202.

Qin T. Y., Noda N. A., 2002, Analysis of three-dimensional crack terminating at an interface using a hypersingular integral equation method. *ASME J. Applied Mechanics* 69(5), 626 – 631

Qin T. Y., Noda N. A., 2003, Stress intensity factors of a rectangular crack meeting a bimaterial interface. *Int. J. Solids Structures* 40(10), 2473-2486

Roy A., Saha T.K., 2000. Weight function for an elliptic crack in an infinite medium. I. Normal loading. *Int J Fract.* 103.227-241.

Tada H. Studies of the crack opening stretch concept in application to several fracture problems. Ph.D dissertation. Lehigh university. June, 1972.

Tracey D. M., Cook T. S., 1977. Analysis of power type singularities using finite elements. *Int. J. Numer. Meth. Engng.* 11, 1225-1233

Westergaard H M. Bearing pressures and cracks. *ASME, Journal of Applied Mechanics, Series A*, 1939, 66;49

Whye T.A., Hui F. 2004. A hypersingular boundary integral method for quasi-static antiplane deformations of an elastic bimaterial with an imperfect and viscoelastic interface. *Engng Comput.* 21, 529-539

Xiao Q. Z, Karihaloo B.L., 2002. Approximate Green's functions for singular and higher order terms of an edge crack in a finite plate. *Engng. Fract. Mech* 69, 959-981